

SME OBSERVATIONS OF $O_2(^1\Delta_g)$ NIGHTGLOW: AN ASSESSMENT OF THE CHEMICAL PRODUCTION MECHANISMS

COLIN D. HOWELL, DIANE V. MICHELANGELI, MARK ALLEN† and YUK L. YUNG
Division of Geological and Planetary Sciences, California Institute of Technology, Pasadena,
CA 91125, U.S.A.

and

RONALD J. THOMAS

Laboratory for Atmospheric and Space Physics, University of Colorado, Boulder, CO 80309, U.S.A.

(Received 5 October 1989)

Abstract—*Solar Mesosphere Explorer (SME)* observations of the 3 a.m. 1.27 μm nightglow at 45°N latitude, averaged over the period 10–31 July 1984, are reported. From the deduced volume emission rates, we derive the $O_2(^1\Delta_g)$ night-time production rates for the 80–100 km altitude range. Utilizing the mean *SME*-acquired 3 p.m. ozone profile for the same latitude and time period and an updated photochemical model, we determine night-time O, O_3 , H, OH, HO_2 , and H_2O_2 profiles. These are used in calculating the rates of reactions which are sufficiently exothermic to produce $O_2(^1\Delta)$ or excited states of OH or HO_2 , which could transfer their energy to O_2 to form $O_2(^1\Delta)$. Of these reactions, most have rates that are quite small compared with the observed night-time $O_2(^1\Delta)$ production rate. For several others, laboratory experiments have found $O_2(^1\Delta)$ yields which are insufficient for simulating the observed $O_2(^1\Delta)$. Using yields of $O_2(^1\Delta)$ based on published laboratory and observational studies, we find that the sum of two reaction sequences can approximate the *SME* measurements: (1) $O + O + M$ and (2) $H + O_3$ followed by $OH^* + O_2$.

INTRODUCTION

First identified as a phenomenon of the terrestrial atmosphere by Yntema (1909), airglow at visible and infrared wavelengths is readily observed, but the processes leading to the emission are not fully understood. In this paper, we shall examine the chemical source of the O_2 (Infrared Atmospheric System: $a^1\Delta_g \rightarrow X^3\Sigma_g^-$) nightglow at 1.27 μm .

Measurements of the 1.27 μm nightglow have been reported most recently by McDade *et al.* (1987a) and Lopez-Moreno *et al.* (1988). Both sets of airglow observations were acquired before local midnight and, consequently, contained an unknown mixture of emission resulting from night-time chemistry and from $O_2(^1\Delta)$ produced during the day by ozone photolysis in the Hartley bands (220–310 nm) (Vallance Jones and Gattinger, 1963). The *Solar Mesosphere Explorer (SME)* satellite measurements of the 1.27 μm emission are for a local time of ~ 3 a.m., sufficiently long after sunset to reveal the intrinsic emission produced at

night by chemical reactions. The complementary *SME* daytime (~ 3 p.m.) airglow measurements, in combination with a photochemical model, allow the inference of key odd-oxygen and odd-hydrogen species profiles. Thus, the *SME* data provide a unique opportunity to explore potential mechanisms for the night-time production of $O_2(^1\Delta)$.

SME MEASUREMENTS OF NIGHT-TIME 1.27 μm EMISSION

A typical *SME* 24-h observing schedule included data acquisition during the daylight portion of five orbits and the night-time part of one orbit. The Near Infrared Spectrometer (NIRS) and the analysis of the daytime 1.27 μm radiances are described in Thomas *et al.* (1984). Interesting night-time observations are the $O_2(^1\Delta)$ emission at 1.27 μm discussed in this paper and the OH(7–5) Meinel band emission analyzed by Le Texier *et al.* (1987, 1989).

The NIRS scans the limb vertically as the *SME* satellite spins. A telescope defines a field-of-view on the limb, 3.3 km high and 33 km wide. The observed limb radiance profile can be compared directly to a model calculation, or inverted to yield a volume emis-

† Also, Earth and Space Sciences Division, Jet Propulsion Laboratory, California Institute of Technology, Pasadena, CA 91109, U.S.A.

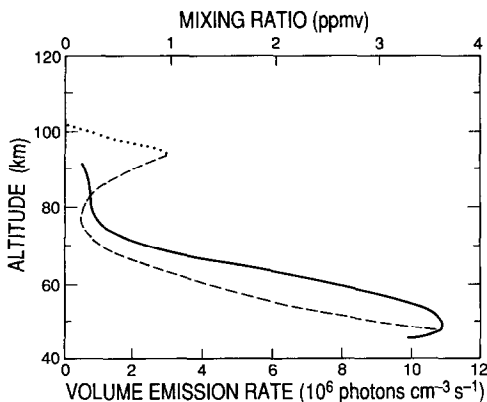


FIG. 1. *SME* DAYTIME (~ 3 p.m.) $1.27 \mu\text{m}$ VOLUME EMISSION RATES (SOLID LINE) AND THE DERIVED O_3 PROFILE (DASHED LINE) FOR 45°N LATITUDE.

The unit for the ozone mixing ratio is parts per million by volume. The limb radiances, from which these results were derived, are averages of all data in the period 10–31 July 1984. The extrapolation of the ozone profile to higher altitudes, as discussed in the text, is indicated by the dotted portion of the curve.

sion rate profile. Since the instrument sensitivity was optimized for the daytime measurements, the signal-to-noise ratio at night is low. In a single scan set (six adjacent scans taken in 1 min), the noise is about 1 MR (1 MR = 10^{12} photons $\text{cm}^{-2} \text{s}^{-1}$), compared with a peak signal of 5 MR. When 32 scan sets have been averaged together, the noise is reduced to about 0.2 MR. Since the spectrometer is detector-noise limited, the noise is constant with altitude and independent of signal.

Another source of error arises from the manner in which the altitude of each observation was determined. For the daylight portions of an orbit, the altitude is derived using the Rayleigh scattering profiles acquired with the *SME* ultraviolet spectrometer and has an uncertainty of 1 km. The altitude scale for the night-time measurements was determined from spacecraft attitude and has an uncertainty of several kilometers. The uncertainty in assignment of altitude will tend to smear the averaged nightglow profile, decreasing the altitude resolution to ~ 5 km.

For the purposes of this paper, we averaged together the available *SME* NIRS radiance data near 45°N latitude for the period 10–31 July 1984. We display, in Fig. 1, the daytime (~ 3 p.m.) $1.27 \mu\text{m}$ volume emission rates. Above 80 km, the O_3 concentration is directly proportional to the emission rate, while below 70 km it is the O_3 mixing ratio that is directly proportional to the emission rate because collisional quenching of $\text{O}_2(^1\Delta)$ becomes important.

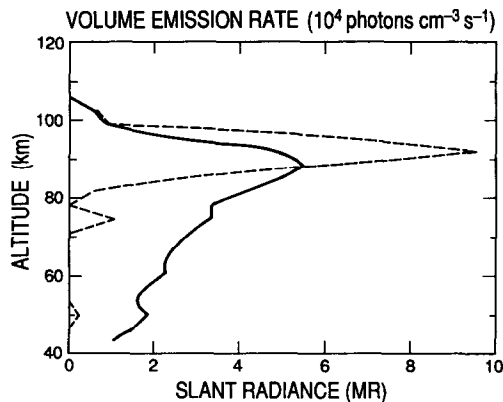


FIG. 2. *SME* NIGHT-TIME (~ 3 a.m.) $1.27 \mu\text{m}$ LIMB RADIANCES (SOLID LINE) AND THE RETRIEVED VOLUME EMISSION RATES (DASHED LINE) FOR 45°N LATITUDE, 10–31 JULY 1984.

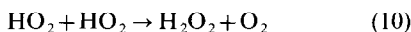
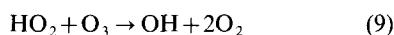
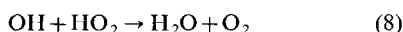
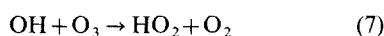
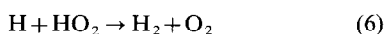
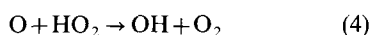
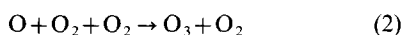
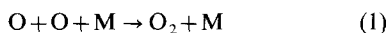
The daytime O_3 profile retrieved from the volume emission rates is shown in Fig. 1 and will be utilized later in this paper to infer night-time profiles of key chemical species. In Fig. 2, we display the averaged night-time (~ 3 a.m.) $1.27 \mu\text{m}$ limb radiances and the volume emission rates derived from these data. The volume emission rate peaks near 92 km and is $\sim 10^5$ photons $\text{cm}^{-3} \text{s}^{-1}$. This is 20% of the daytime value at the same altitude (cf. Fig. 1). Above the altitude of peak emission, the uncertainty in the retrieved volume emission rate is $\sim 25\%$; below the peak the uncertainty is $\pm 2 \times 10^4$ photons $\text{cm}^{-3} \text{s}^{-1}$. The objective of the rest of this paper is the identification of the chemical sources of the night-time $\text{O}_2(^1\Delta)$ $1.27 \mu\text{m}$ emission.

POTENTIAL NIGHT-TIME CHEMICAL SOURCES OF $\text{O}_2(^1\Delta)$

The daytime $1.27 \mu\text{m}$ volume emission rate is five times larger than the night-time value near the night-time peak at 92 km. Although the radiative lifetime of $\text{O}_2(^1\Delta)$ is long (1.06 h; Badger *et al.*, 1965), at 3 a.m. (~ 6.5 h after sunset at the mesopause) the remnant dayglow is $< 0.2\%$ of the 3 p.m. value and only $\sim 1\%$ of the 92 km nightglow. Since photolysis of O_3 is the dominant source of daytime $\text{O}_2(^1\Delta)$ and O_3 abundances near 90 km are relatively constant during the daylight period (see Allen *et al.*, 1984), we have assumed that the observed 3 p.m. volume emission rates are constant until sunset. Near 80 km the remnant dayglow is a larger fraction of the 3 a.m. nightglow, but it is only 3% of the nightglow and therefore still unimportant. Consequently, we assume that all of the observed nightglow is the result of chemical

reactions occurring near 3 a.m. at the altitudes of the observed emission.

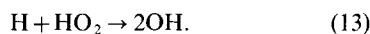
The lowest ro-vibrational level in the O₂(*a*¹Δ_g) state is 0.98 eV above the ground ro-vibrational level of the O₂(*X*³Σ_g⁻) state. A number of the chemical reactions involving hydrogen- and oxygen-containing species that are likely to occur near the night-time mesopause have O₂ as a product and are exothermic by more than 1 eV. Utilizing the gas phase enthalpy data in DeMore *et al.* (1987), we have identified these reactions, which energetically could produce O₂(¹Δ) or higher excited states of O₂ [which through subsequent collision with O₂ generate O₂(¹Δ)]:



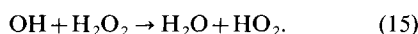
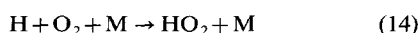
In many of the above reactions, product species other than O₂ could be in an excited state with more than 1 eV of energy and through subsequent collisions transfer energy to form O₂(¹Δ). The O₂(¹Δ) may be created in the reaction between atomic O and product OH* (*v* ≥ 1):



In addition, product OH* in vibrational levels *v* ≥ 3 or electronically-excited product HO₂* may be quenched by collisions with the ambient O₂ by a mechanism resulting in the formation of O₂(¹Δ). Product OH* is energetically possible in reactions (4), (5), and (9) and in



Product HO₂* is energetically possible in reaction (7) and in



To evaluate the possible contributions of reactions (1)–(15) to the observed 1.27 μm emission, we need

to estimate their reaction rates at 3 a.m. This in turn requires knowledge of the relevant species abundances at the epoch and location of the *SME* observations. In the next section we discuss our derivation of the 3 a.m. O, O₃, H, OH, HO₂, and H₂O₂ profiles.

CALCULATION OF NIGHT-TIME PROFILES OF KEY OXYGEN- AND HYDROGEN-CONTAINING SPECIES

The Caltech/JPL one-dimensional time-dependent photochemical model (described in Allen *et al.*, 1981, 1984; update: preprint, 1989) was used, along with the mean daytime (~ 15:00 L.T.) O₃ profile corresponding to the nightglow measurements being analyzed, to calculate the concentrations of the important oxygen- and hydrogen-containing species in the lower thermosphere (≥ 80 km). The atmospheric parameters of temperature and pressure were taken from values in Houghton (1977) for June at 40°N latitude. The altitude scale, in nearly 2 km intervals between 50 and 105 km, was calculated assuming hydrostatic equilibrium. We ran the photochemical model through several diurnal cycles (with the radiation field varying as appropriate for a spherical atmosphere) until species abundances separated by 24 h agreed to within a few percent. This standard model yields 3 p.m. O₃ abundances significantly smaller than the *SME* measured distribution below 80 km, with the reverse result at higher altitudes. This is discussed in detail by Clancy *et al.* (1987). To improve the model simulation of the *SME* profile, we reduced the prescribed eddy diffusion profile (see discussion in Strobel *et al.*, 1987); increased O₂ photocross-sections by 40%, decreased O₃ photocross-sections by 10%, increased the reaction rate constant for OH + HO₂ to the upper limits defined by the uncertainties reported by Keyser (1988) (see discussion in Clancy *et al.*, 1987 and Froidevaux *et al.*, 1989); and set the lower boundary condition (50 km) for H₂O to 6 ppmv. An improvement in the model fit to observations resulted between 50 and 80 km, but above 80 km the calculated values are still higher than the *SME* data. We feel, however, that above 80 km the relative diurnal variation of species abundances and the profiles of hydrogen-containing species as computed by the modified model are reasonable for the epoch of the *SME* observations. Therefore, the 3 a.m. abundances of H, OH, HO₂, and H₂O₂ were taken directly from the output of the modified photochemical model. These profiles are displayed in Fig. 3a. At 90 km, where atomic H is long-lived, the calculated atomic H concentration is in good agreement with the measurements of Sharp and Kita (1987).

Since the *SME* O₃ profile above 80 km is not repro-

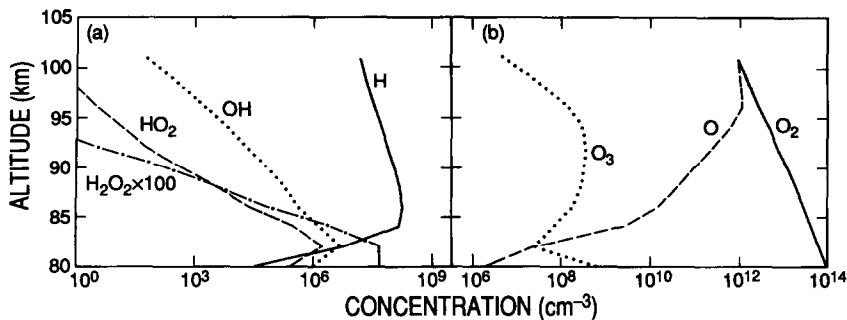


FIG. 3. SPECIES CONCENTRATIONS DEDUCED FOR 3 a.m. AS DESCRIBED IN THE TEXT: (a) H, OH, HO₂, AND H₂O₂, (b) O, O₂, AND O₃.

duced in the model calculations, we work directly from the O₃ observations to determine the appropriate night-time atomic O and O₃ distributions; because the nightglow extends over the range 80–100 km (Fig. 2) and the retrieved daytime O₃ profile extends only up to ~93 km (Fig. 1), we extrapolated the daytime density profile to 100 km using the variation with altitude calculated by the modified model (the extrapolation is displayed in Fig. 1 in units of mixing ratio). The daytime atomic O profile was derived from the daytime *SME* O₃ by utilizing the daylight steady-state relationship between atomic O and O₃ (Allen *et al.*, 1984),

$$[\text{O}] = \frac{(J_{\text{O}_3} + k_5[\text{H}])[\text{O}_3]}{(k_2[\text{O}_2] + k_{\text{N}_2}[\text{N}_2])[\text{O}_2]}, \quad (16)$$

where J_{O_3} is the O₃ photodissociation rate constant and k_{N_2} is the O₃ recombination rate constant for N₂ as a third body. The square brackets indicate volume densities. To obtain the 3 a.m. atomic O profile, we scaled the 3 p.m. atomic O abundances calculated from (16) by the 3 a.m./3 p.m. atomic O abundance ratio computed by the modified photochemical model. In turn, from these atomic O values, the night-time O₃ distribution was calculated from the night-time version of the photochemical steady-state expression of equation (1) in Allen *et al.* (1984):

$$[\text{O}_3] = \frac{[\text{O}][\text{O}_2](k_2[\text{O}_2] + k_{\text{N}_2}[\text{N}_2])}{k_3[\text{O}] + k_5[\text{H}]}. \quad (17)$$

The 3 a.m. atomic O and O₃ concentrations, along with the assumed O₂ profile, are shown in Fig. 3b. The atomic O profile is similar to the summer midlatitude profile from *Aladdin 74* (Trinks *et al.*, 1978), the differences being within the range of natural fluctuations of the atmosphere. As discussed in Allen (1986), the above simple steady-state photochemical relationships between atomic O and O₃ do not repro-

duce observed [O]/[O₃] values in the lower thermosphere. However the discrepancy is most severe above 100 km. Moreover, our use of the photochemical relationship twice, starting with 3 p.m. O₃ and ending with 3 a.m. O₃, should minimize the error in the 3 a.m. O₃ profile due to possible uncertainties in thermospheric odd-oxygen chemistry. The approach outlined in this section for deriving the night-time species abundances, necessary for later calculations of the potential chemical sources of late night O₂(¹Δ), attempts to extract as much information as possible from the available 3 p.m. *SME* O₃ measurements.

SIMULATION OF NIGHT-TIME O₂(¹Δ) PRODUCTION

The decay of O₂(¹Δ) is the result of (1) the spontaneous emission of a 1.27 μm photon, with a rate constant k_r ($= 2.58 \times 10^{-4} \text{ s}^{-1}$) or (2) quenching upon collision with O₂, with a rate constant k_c [$= 2.22 \times 10^{-18} (T/300)^{0.78} \text{ cm}^3 \text{ s}^{-1}$] (see Thomas *et al.*, 1984, and references therein). Quenching by collision with N₂ is negligible. The total O₂(¹Δ) loss rate L at 3 a.m. can be deduced from the observed volume emission rate V ($= k_r[\text{O}_2(\text{}^1\Delta)]$) through the expression

$$L = \left(1 + \frac{k_c[\text{O}_2]}{k_r}\right)V. \quad (18)$$

Since the remnant of the daytime O₂(¹Δ) is negligible, we shall assume that the O₂(¹Δ) abundance is in steady-state and the total O₂(¹Δ) production rate P is equal to L .

Upon comparing the altitude-varying values of P which we have derived from the volume emission rate and the rates of reactions potentially producing O₂(¹Δ) directly or indirectly, we find that many of these reactions cannot make significant contributions to the observed nightglow (reactions rates $\lesssim 10\%$ of P at the corresponding altitude), even when a 100%

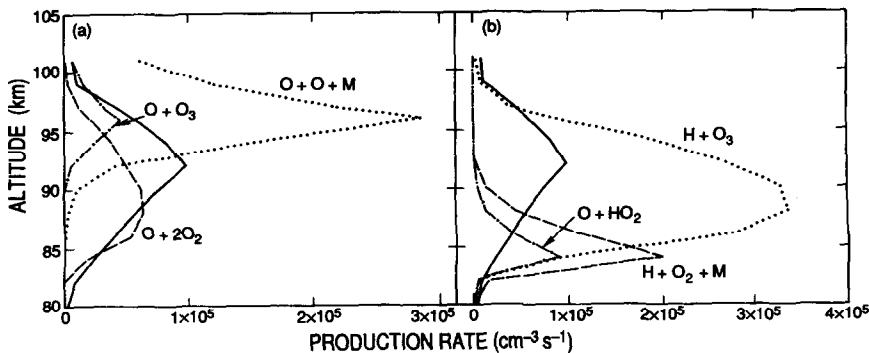


FIG. 4. CALCULATED RATES OF REACTIONS POTENTIALLY YIELDING O₂(¹Δ) EITHER DIRECTLY OR INDIRECTLY COMPARED WITH THE COMPUTED PRODUCTION RATE OF O₂(¹Δ) (SOLID LINE). Calculations are for 3 a.m. (a) O+O+M, O+2O₂ and O+O₃. (b) H+O₂+M, H+O₃, and O+HO₂.

yield of O₂(¹Δ) is assumed. Reactions (6)–(11), (13), and (15) are in this category and will not be considered further. The potential importance of reactions (1)–(5) and (14) for producing the nightglow is illustrated in Fig. 4 in which rates of these reactions are compared with our calculated O₂(¹Δ) production profile (*P*). We note from this figure that the rates of (4) and (14) peak near 84 km and therefore could only effectively contribute to the nightglow in its low altitude tail; as such, these two reactions are not useful candidates for the major portion of the O₂(¹Δ) production rate. One interesting possibility that our analysis precludes is the resonance quenching of HO₂* by O₂ to be an important source of O₂(¹Δ).

Of the remaining reactions, several can make significant contributions to the O₂(¹Δ) production rate only if their efficiency for forming O₂(¹Δ), directly or indirectly, is nearly 100%. Unfortunately, laboratory investigations of O₂(¹Δ) yields are non-existent or incomplete for many reactions. For example, no relevant laboratory data exist for (2). However, since a product of (2) is O₃, the excess energy is expected to reside initially in O₃. Pumping of O₂(¹Δ) during the collisional quenching of excited O₃ is not thought to be highly efficient (Leu, private communication, 1988). On the other hand, some useful laboratory measurements exist for (3) and (5). Washida *et al.* (1980) find upper limits for the yield of O₂(¹Δ) in the reactions of O+O₃ (3), and H+O₃ (5), to be 6 and 0.1%, respectively, at room temperature. It therefore seems that (2), (3), and (5) can be eliminated as direct sources of O₂(¹Δ). Laboratory experiments, however, cannot preclude the possibilities of these reactions yielding O₂(¹Δ) through indirect mechanisms under atmospheric conditions, which were not simulated in the experiments.

However, (5) is the primary atmospheric source of OH*, yielding OH* in excited vibrational levels $v = 4-9$ (most recent laboratory results reported in Oho-yama *et al.*, 1985). The airglow from OH* was first reported by Meinel (1950). Reaction (12) with the plentiful atomic O might then be an effective source of the 1.27 μm nightglow. We estimate an upper limit to (12) by first calculating an upper limit to the concentration profile of OH*. Assuming OH* is in steady-state and (5) has unit efficiency for produced OH* (see for example, McDade *et al.*, 1987b), we equate the reaction rate for (5), R_5 , to the collisional quenching rate for OH* ($v = 1$), with a rate constant k_{19} ,



yielding

$$[\text{OH}^*] = \frac{R_5}{k_{19}[\text{M}]}. \quad (20)$$

In this approximation, radiative and collisional processes result in rapid redistribution to the lowest excited vibrational level, from where collisional de-excitation predominates over radiative decay (see "collisional cascade model" in McDade and Llewellyn, 1987), so that the only loss of OH* ($v \geq 1$) is by reaction (19). The resulting vertical profile of OH* densities is used in calculating the rate of (12). Adopting the values $k_{12} = 4 \times 10^{-11} \text{ cm}^3 \text{ s}^{-1}$ and $k_{19} = 8 \times 10^{-13} \text{ cm}^3 \text{ s}^{-1}$ (Llewellyn and Solheim, 1978; Llewellyn *et al.*, 1978), we find that the production of O₂(¹Δ) by (12) is equal to our calculated values of *P* above ~ 95 km if the yield for O₂(¹Δ) is ~ 22%. Reaction (12) has been suggested as a significant source of O₂(¹Δ) in several previous investigations of airglow observations, most recently, by

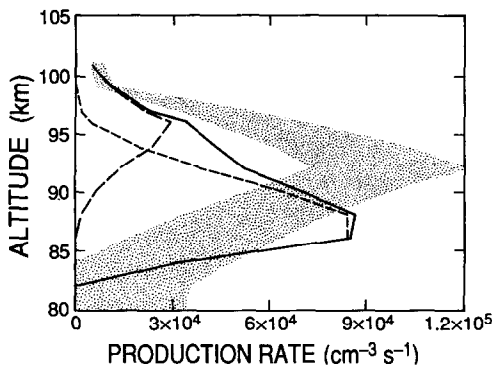


FIG. 5. THE PRODUCTION RATE OF $O_2(^1\Delta)$ DEDUCED FROM *SME* $1.27 \mu\text{m}$ NIGHTGLOW MEASUREMENTS (SHADED AREA DEFINED BY UNCERTAINTIES IN P) COMPARED WITH THE RATE FOR REACTION (1) MULTIPLIED BY $f_1(z)$ (LONG DASHED LINE) AND THE RATE FOR REACTION (5) MULTIPLIED BY $f_5(z)$ (SHORT DASHED LINE) (SEE TEXT FOR DISCUSSION OF EFFICIENCY FACTORS).

The sum of these two components, the total model production rate of $O_2(^1\Delta)$, is indicated with a solid line.

Lopez-Moreno *et al.* (1988). The $O_2(^1\Delta)$ yields in these other works were comparable to or greater than our value. However, in their recently published paper, Lunt *et al.* (1988) conclude that the yield of $O_2(^1\Delta)$ in (12) is only 2.5%, thus apparently also eliminating this channel as an important source of the nightglow measured by the *SME*.

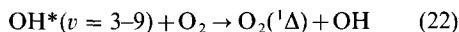
An efficient source of $O_2(^1\Delta)$ in the laboratory is (1), the recombination of atomic O. Ali *et al.* (1986) report that the direct yield of $O_2(^1\Delta)$ is 7%, while the total yield, including indirect channels involving quenching of higher excited states of O_2 , is as much as 75%. They find that the indirect yield is due to the presence of O_2 , but is suppressed by atomic O. Following equation (9) of Ali *et al.* (1986), we multiply the altitude-varying rate of (1) by an efficiency factor f_1 , which varies with altitude as a result of the change with altitude of the atomic O to O_2 abundance ratio:

$$f_1(z) = 0.07 + \frac{0.7}{50[\text{O}]/[\text{O}_2] + 1}. \quad (21)$$

As shown in Fig. 5, the rate of $O_2(^1\Delta)$ formation thus calculated [$= f_1(z)R_1(z)$] is comparable to the $O_2(^1\Delta)$ production rate deduced from observations above ~ 97 km. Above 97 km, $f_1(z)$ is < 0.1 , whereas near the peak of P near 92 km $f_1(z)$ is ~ 0.6 . Therefore, the rapid falloff with decreasing altitude in the production of $O_2(^1\Delta)$ due to (1) is directly the result of the rapid decrease with decreasing altitude of the atomic O abundance (see Fig. 3b). Our conclusion

that the yield of $O_2(^1\Delta)$ in (1) is relatively small at the altitudes where (1) can contribute to $O_2(^1\Delta)$ formation is in disagreement with the analysis by McDade *et al.* (1987a) of their observation which suggests $O_2(^1\Delta)$ yields $\geq 50\%$ and the analysis by Lopez-Moreno *et al.* (1988) of their own observations which suggests a yield of 75%. On the other hand, Bates (1988) deduces from available measurements an effective yield of only 28%. Clearly, the necessary yield for $O_2(^1\Delta)$ production derived from model analyses of $1.27 \mu\text{m}$ measurements will vary depending on the accuracy of the atomic O profile observed simultaneously or deduced in a variety of ways. How close the temperature profile utilized in the calculations is to the actual temperatures, which often have not been measured simultaneously with the acquisition of the airglow data, will also affect the derived yield. Since Lopez-Moreno *et al.* (1988) do not know precisely the contribution to their $1.27 \mu\text{m}$ nightglow measurements from the dayglow remnant, any underestimate of the magnitude of this remnant will require an increase in the necessary $O_2(^1\Delta)$ yield in (1) to reproduce the observed nightglow.

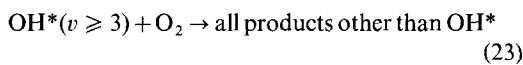
We are still missing the source of $O_2(^1\Delta)$ production at and below the peak at 92 km. McDade and Llewellyn (1987) (also, McDade *et al.*, 1987b) conclude that the vibrational population of the observed OH^* nightglow could be modeled equally well either assuming that collisional quenching of $\text{OH}^*(v)$ leads to population of $\text{OH}^*(v' < v)$ ("collisional cascade model") or assuming that collisional processes result in a net loss of OH^* ("sudden death model"). We have shown above that the first possibility does not result in a rate of $O_2(^1\Delta)$ production via (12) that is sufficient to reproduce P . We now consider whether the second possibility of McDade and Llewellyn (1987), the "sudden death" assumption, may lead to a large rate of $O_2(^1\Delta)$ formation. The reaction



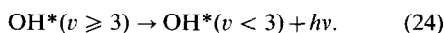
is exothermic. The possibility of (22) being a source of $O_2(^1\Delta)$ in the upper atmosphere has been discussed by Han *et al.* (1973), Thomas *et al.* (1984), and Wayne (1984). Finlayson-Pitts and Kleindienst (1981) found that the rate constant for quenching of $\text{OH}^*(v = 9)$ by O_2 is 20 times larger than the rate constant for quenching by N_2 . They suggest that the enhanced effectiveness of O_2 relative to N_2 might be understood as being the result of resonant energy transfer; according to these authors, $\text{O}_2(b^1\Sigma)$ could be the product, although they have no information as to which excited states of O_2 are the products. In the laboratory experiments of Lunt *et al.* (1988), (22) is not a significant source of the measured $O_2(^1\Delta)$ compared with other

reactions that were occurring simultaneously. However, their experimental conditions were not chosen to simulate thermospheric conditions and species abundances, so we do not believe that a definitive experimental test of (22) has yet been published. Interestingly, Llewellyn and Solheim (1978) found a correlation between their measurements of OH* and O₂(¹Δ) emission, as would be expected if (22) were to be the main contributor to O₂(¹Δ).

The rate-controlling step in the O₂(¹Δ) formation mechanism consisting of (5) followed by (22) is the reaction rate for (5), R_5 . The altitude-dependent yield of O₂(¹Δ) for this overall sequence, f_5 , reflects the competition between



and



Consequently,

$$f_5 = \frac{f_{22}k_{23}[\text{O}_2]}{A_{24} + k_{23}[\text{O}_2]}, \quad (25)$$

where $k_{22} = f_{22}k_{23}$ and A_{24} is the radiative transition probability for OH* emission. From their analysis using the "sudden death model", McDade and Llewellyn (1987) derive a value for k_{23}/A_{24} of $\sim 5 \times 10^{-14}$ cm³ for $v = 7-9$ and smaller values for $v < 7$. We have assumed here that atomic O is not an effective quencher of OH* compared with O₂ since $[\text{O}]/[\text{O}_2]$ is ≥ 1 only ≥ 100 km and this ratio decreases rapidly with decreasing altitude (~ 0.01 at 90 km).

Since (5) yields OH* in the higher vibrational levels, we adopt the value for k_{23}/A_{24} appropriate for these levels and find that the profile of f_5R_5 that best matches P occurs when half of the quenching of OH* by O₂ yields O₂(¹Δ) ($f_{22} \sim 0.5$). These results are shown in Fig. 5. The total profile is similar to the observed emission, but the peak model production of O₂(¹Δ) is ~ 5 km below the apparent peak production level. Near 95 km, the model production rate is $\sim 30\%$ smaller than the range in values inferred from *SME* observations. Near 86 km, the model results are $\sim 30\%$ larger than the inferred values. As discussed earlier, the model results are quite sensitive to the species profiles shown in Fig. 3. Differences between the calculated and actual values of the important atmospheric species, such as atomic H, could easily be of the order of 30%, thus explaining the discrepancy between the model and inferred O₂(¹Δ) production rates. The reader should note that, in reaction (22), reduction of OH* by

three vibrational levels is energetically sufficient to excite O₂(¹Δ) and still leave OH* in a highly vibrationally-excited state. This scenario is not explored in McDade and Llewellyn (1987) and would result in slightly different calculated production rates for O₂(¹Δ).

CONCLUSIONS

The *SME* observations of the 1.27 μm nightglow provide a unique opportunity to study the late night chemical sources of O₂(¹Δ_g). Acquired at a local time of 3:00, more than 6 h after sunset, these data are relatively free of residual 1.27 μm dayglow. We have deduced from the nightglow measurements the mean vertical distribution of O₂(¹Δ) production for 45°N latitude in the period 10–31 July 1984. Of the reaction mechanisms that are sufficiently exothermic to produce O₂(¹Δ), we find that only direct and/or indirect production from O+O+M and production from the sequence H+O₃ → OH*+O₂, followed by OH*+O₂ → OH+O₂(¹Δ), have rates large enough to reproduce the inferred production rates. Altitude-dependent yields for O₂(¹Δ) in each mechanism were based on laboratory experiments and/or detailed analyses of airglow data. The total O₂(¹Δ) production rate thus calculated approximates the profile inferred from *SME* observations.

It is interesting to consider whether the chemical sources of O₂(¹Δ) at night could also be significant contributors to the daytime 1.27 μm emissions. Atomic O and H abundances above 80 km do not have much diurnal variation and O₃ is less abundant during the day than at night (Allen *et al.*, 1984). Thus, the key reactions we have identified remain constant or even decrease from night to day. Since the dayglow at 1.27 μm at 92 km is five times the nightglow, the chemical sources of the nightglow will contribute little to the daytime O₂(¹Δ) formation rate.

The deduced yields for O₂(¹Δ) in the reactions O+O+M and H+O₃ → OH*+O₂ [followed by OH*+O₂ → OH+O₂(¹Δ)] are quite dependent on the key species and temperature profiles adopted in the calculations. The accuracy of these yields is a function of the degree to which these profiles appropriately represent the atmosphere for the period of the *SME* measurements. Simultaneous observations of O₂(¹Δ) and atomic O or O₂(¹Δ) and OH* have been reported in the literature. Generally, these measurements were made in the early night (before midnight). It is clear from our analysis that significant further progress in understanding the mechanisms for night-time O₂(¹Δ) production will be made upon acquiring late night (post-midnight) simultaneous

profiles of $O_2(^1\Delta)$, atomic O, O_3 , atomic H, OH^* , and temperature.

While we have tried to identify the specific reactions leading to the formation of $O_2(^1\Delta)$, we suggest a more general conclusion of our work is that the ultimate source of excitation is the chemical energy stored in atomic O. The upper part of the 1.27 μm nightglow layer is directly due to atomic O recombination. The lower portion of the nightglow profile is a consequence of the recombination of atomic O with O_2 to form O_3 . Since O_3 is in steady-state at night, this recombination reaction is balanced by the reaction $H + O_3$, the main O_3 loss process (Allen *et al.*, 1984). In this context, the sequence $H + O_3$, followed by $OH^* + O_2$, is one likely means of transferring the energy of O_3 recombination to $O_2(^1\Delta)$. A similar profile of $O_2(^1\Delta)$ production would result if $O_2(^1\Delta)$ were produced directly in the process of O_3 recombination. Here also simultaneous measurements of temperature and key species (particularly, atomic O) would be needed to distinguish the specific excitation mechanism.

Finally, we note that the bulk of $O_2(^1\Delta)$ production in our calculations is due to the reaction mechanism $H + O_3$, followed by $OH^* + O_2$. We have previously pointed out that this mechanism is also capable of forming $O_2(b^1\Sigma)$. A comparison of night-time observations of $O_2(^1\Sigma)$ (Witt *et al.*, 1984; McDade *et al.*, 1986) and the *SME* measurements of $O_2(^1\Delta)$ suggests that the yield of $O_2(^1\Sigma)$ in the reaction $OH^* + O_2$ would need to be $\sim 5\%$. One way to test the hypothesis of whether $O_2(^1\Delta)$ and $O_2(^1\Sigma)$ emissions are due to the same mechanism would be to monitor the correlation between them.

Acknowledgements—We gratefully acknowledge assistance received from R. T. Clancy and M. T. Leu. This work was supported by NASA grant NAGW-890 to the University of Colorado and NASA grant NAGW-413 to the California Institute of Technology. C. D. Howell was supported by a California Institute of Technology Summer Undergraduate Research Fellowship.

REFERENCES

- Ali, A. A., Ogryzlo, E. A., Shen, Y. Q. and Wassell, P. T. (1986) The formation of $O_2(a^1\Delta_g)$ in homogeneous and heterogeneous atom recombination. *Can J. Chem.* **64**, 1614.
- Allen, M. (1986) A new source of ozone in the terrestrial upper atmosphere? *J. geophys. Res.* **91**, 2844.
- Allen, M., Lunine, J. I. and Yung, Y. L. (1984) The vertical distribution of ozone in the mesosphere and lower thermosphere. *J. geophys. Res.* **89**, 4841.
- Allen, M., Yung, Y. L. and Waters, J. W. (1981) Vertical transport and photochemistry in the terrestrial mesosphere and lower thermosphere (50–120 km). *J. geophys. Res.* **86**, 3617.
- Badger, R. M., Wright, A. C. and Whitlock, R. F. (1965) Absolute intensities of the discrete and continuous absorption bands of oxygen gas at 1.26 and 1.065 μ and the radiative lifetime of the $^1\Delta_g$ state of oxygen. *J. chem. Phys.* **43**, 4345.
- Bates, D. R. (1988) Excitation and quenching of the oxygen bands in the nightglow. *Planet. Space Sci.* **36**, 875.
- Clancy, R. T., Rusch, D. W., Thomas, R. J., Allen, M. and Eckman, R. S. (1987) Model ozone photochemistry on the basis of *Solar Mesosphere Explorer* mesospheric observations. *J. geophys. Res.* **92**, 3067.
- DeMore, W. B., Molina, M. J., Sanders, S. P., Golden, D. M., Hampson, R. F., Kurylo, M. J., Howard, C. J. and Ravishankara, A. R. (1987) Chemical kinetics and photochemical data for use in stratospheric modeling. *JPL Publ.*, JPL 87-41.
- Finlayson-Pitts, B. J. and Kleindienst, T. E. (1981) The reaction of hydrogen atoms with ozone and source of vibrationally excited $OH(X^2\Pi)_{v=2}$ for kinetic studies. *J. chem. Phys.* **74**, 5643.
- Froidevaux, L., Allen, M., Berman, S. and Daughton, A. (1989) The mean ozone profile and its temperature sensitivity in the upper stratosphere and lower mesosphere: an analysis of LIMS observations. *J. geophys. Res.* **94**, 6389.
- Han, R. Y., Megill, L. R. and Wyatt, C. L. (1973) Rocket observation of the equatorial $O_2(^1\Delta_g)$ emission after sunset. *J. geophys. Res.* **78**, 6140.
- Houghton, J. T. (1977) *The Physics of Atmospheres*, p. 173. Cambridge University Press, Cambridge.
- Keyser, L. F. (1988) Kinetics of the reaction $OH + HO_2 \rightarrow H_2O + O_2$ from 254 to 382 K. *J. phys. Chem.* **92**, 1193.
- Le Texier, H., Solomon, S. and Garcia, R. R. (1987) Seasonal variability of the Meinel bands. *Planet. Space Sci.* **35**, 977.
- Le Texier, H., Solomon, S., Thomas, R. J. and Garcia, R. R. (1989) OH^* (7–5) Meinel band dayglow and nightglow measured by the *SME* limb scanning Near Infrared Spectrometer: comparison of the observed seasonable variability with two-dimensional model simulations. *Ann. Geophys.* **7**, 365.
- Llewellyn, E. J. and Solheim, B. H. (1978) The excitation of the infrared atmospheric oxygen bands in the nightglow. *Planet. Space Sci.* **26**, 533.
- Llewellyn, E. J., Long, B. H. and Solheim, B. H. (1978) The quenching of OH^* in the atmosphere. *Planet. Space Sci.* **26**, 525.
- Lopez-Moreno, J. J., Rodrigo, R., Moreno, F., Lopez-Puertas, M. and Molina, A. (1988) Rocket measurements of O_2 Infrared Atmospheric System in the nightglow. *Planet. Space Sci.* **36**, 459.
- Lunt, S. T., Marston, G. and Wayne, R. P. (1988) The formation of $O_2(a^1\Delta_g)$ and vibrationally excited OH in the reaction between O atoms and HO_2 species. *J. chem. Soc. Faraday Trans. 2* **84**, 899.
- McDade, I. C. and Llewellyn, E. J. (1987) Kinetic parameters related to sources and sinks of vibrationally excited OH in the nightglow. *J. geophys. Res.* **92**, 7643.
- McDade, I. C., Murtagh, D. P., Greer, R. G. H., Dickinson, P. H. G., Witt, G., Stegman, J., Llewellyn, E. J., Thomas, L. and Jenkins, D. B. (1986) ETON2: quenching parameters for the proposed precursors of $O_2(b^1\Sigma_g^+)$ and $O(^1S)$ in the terrestrial nightglow. *Planet. Space Sci.* **34**, 789.
- McDade, I. C., Llewellyn, E. J., Greer, R. G. H. and Murtagh, D. P. (1987a) ETON6: a rocket measurement of the O_2

- Infrared Atmospheric (0-0) band in the nightglow. *Planet. Space Sci.* **35**, 1541.
- McDade, I. C., Llewellyn, E. J., Murtagh, D. P. and Greer, R. G. H. (1987b) ETON5: simultaneous rocket measurements of the OH Meinel Δv = 2 sequence and (8,3) band emission profiles in the nightglow. *Planet. Space Sci.* **35**, 1137.
- Meinel, A. B. (1950) OH emission bands in the spectrum of the night sky, I. *Astrophys. J.* **111**, 555.
- Ohoyama, H., Kasai, T., Yoshimura, Y., Kimura, H. and Kuwata, K. (1985) Initial distribution of vibration of the OH radicals produced in the H+O₃ → OH(X²Π_{1/2,3/2})+O₂ reaction. Chemiluminescence by a crossed beam technique. *Chem. Phys. Lett.* **118**, 263.
- Sharp, W. E. and Kita, D. (1987) *In situ* measurement of atomic hydrogen in the upper mesosphere. *J. geophys. Res.* **92**, 4319.
- Strobel, D. F., Summers, M. E., Bevilacqua, R. M., DeLand, M. T. and Allen, M. (1987) Vertical constituent transport in the mesosphere. *J. geophys. Res.* **92**, 6691.
- Thomas, R. J., Barth, C. A., Rusch, D. W. and Sanders, R. W. (1984) Solar Mesosphere Explorer Near-Infrared Spectrometer: measurements of 1.27 μ radiance and the inference of mesospheric ozone. *J. geophys. Res.* **89**, 9569.
- Trinks, H., Offermann, D., Zahn, U. von and Steinhauer, C. (1978) Neutral composition measurements between 90- and 220-km altitudes by rocket-borne mass spectrometer. *J. geophys. Res.* **83**, 2169.
- Vallance Jones, A. and Gattinger, R. L. (1963) The variations and excitation mechanism of the 1.58 μm ¹Δ_g-³Σ_g⁻ twilight airglow band. *Planet. Space Sci.* **11**, 961.
- Washida, N., Akimoto, H. and Okuda, M. (1980) Is O₂^{*}(a¹Δ_g) formed in the O+O₃, H+O₃, and NO+O₃ reactions? *Bull. chem. Soc. Japan* **53**, 3496.
- Wayne, R. P. (1984) Singlet oxygen airglow. *J. Photochem.* **25**, 345.
- Witt, G., Stegman, J., Murtagh, D. P., McDade, I. C., Greer, R. G. H., Dickinson, P. H. G. and Jenkins, D. B. (1984) Collisional energy transfer and the excitation of O₂(b¹Σ_g⁺) in the atmosphere. *J. Photochem.* **25**, 365.
- Yntema, L. (1909) On the brightness of the sky and the total amount of starlight. *Publ. Astr. Lab. Groningen* **22**, 1.